Advanced Review

Hyperspectral microscopy as an analytical tool for nanomaterials

Gary A. Roth, Sahil Tahiliani, Nicole M. Neu-Baker and Sara A. Brenner*

Hyperspectral microscopy is an advanced visualization technique that combines hyperspectral imaging with state-of-the-art optics and computer software to enable the rapid identification of materials at the micro- and nanoscales. Achieving this level of resolution has traditionally required time-consuming and costly electron microscopy techniques. While hyperspectral microscopy has already been applied to the analysis of bulk materials and biologicals, it shows extraordinary promise as an analytical tool to locate individual nanoparticles and aggregates in complex samples through rapid optical and spectroscopic identification. This technique can be used to not only screen for the presence of nanomaterials, but also to locate, identify, and characterize them. It could also be used to identify a subset of samples that would then move on for further analysis via other advanced metrology. This review will describe the science and origins of hyperspectral microscopy, examine current and emerging applications in life science, and examine potential applications of this technology that could improve research efficiency or lead to novel discoveries.

How to cite this article:
WIREs Nanomed Nanobiotechnol 2015, 7:565–579. doi: 10.1002/wnan.1330

INTRODUCTION

Nanotechnology is becoming ubiquitous in daily life as applications of advanced materials engineered at the nanoscale range from computers and cell phones to clothing and sporting goods. Nanotechnology involves the use or creation of engineered nanomaterials, including nanoparticles (NPs), which are structures with at least one spatial dimension less than 100 nanometers. The properties of nanomaterials vary considerably with only minor changes in characteristics such as size and concentration, which implies a need for precise and accurate measurement of these properties. The unique characteristics of engineered nanomaterials present several analytical challenges: their small size makes them difficult to locate, characterize, and quantify. Existing methods, such as transmission electron microscopy (TEM), often require considerable time and resources, where preparation and analysis of a single sample may require several hours. Other methods, such as inductively coupled plasma-mass spectrometry (ICP-MS), result in the loss of information regarding certain characteristics in order to precisely and accurately quantify others; e.g., information on size and morphology is sacrificed to measure mass concentration. Unfortunately, in fields where large numbers of samples must be analyzed (such as environmental monitoring and toxicity screening), the use of such intensive techniques is cost-prohibitive. Consequently, new techniques are needed that can either replace the more burdensome methods or act as screening techniques to minimize more resource-intensive analysis.

Hyperspectral microscopy is one technique that is being developed and explored to address current analytical challenges for nanoscale materials. This technique combines hyperspectral imaging (HSI) with advanced optics, typically focusing on specialized dark-field reflectance systems. Numerous publications have demonstrated the technique's effectiveness in a wide range of applications, including fabricating materials and analysis of biological and environmental

*Correspondence to: sbrenner@sunycnse.com

College of Nanoscale Science, Nanobioscience Constellation, State University of New York (SUNY) Polytechnic Institute, New York, NY, USA

Conflict of interest: The authors have declared no conflicts of interest for this article.

samples. HSI has also been performed on certain samples as a potential method for detecting NP state in biological systems. HSI collects characteristic spectral profile data (analogous to that provided by typical spectrophotometry) of infrared and visible light reflected by samples that uniquely identify materials of interest.

To date, no comprehensive review of the literature has been published regarding the use of hyperspectral microscopy for the analysis of nanomaterials. This review provides an overview of the current applications of this technology as an analytical tool or advanced screening method for nanomaterials.

THE SCIENCE OF HSI

HSI is a technique that was first fully realized and implemented in NASA's airborne visible/infrared imaging spectrometer. The principle is to combine spectrophotometry and imaging: instead of taking a single photograph with a single dominant wavelength per pixel, advanced optics and algorithms allow the capture of an entire spectrum per pixel. Since this adds another dimension to an otherwise two-dimensional image, a hyperspectral image is sometimes referred to as a data cube. By collecting spectra of reference materials, it is possible to correlate these reference spectra to a hyperspectral image to identify specific materials of interest in the image. This forms the basis of the technique and its primary advantage: the ability to simultaneously image diverse and heterogeneous samples and identify materials present.[1] The term 'hyperspectral', rather than just 'spectral', refers to the range of wavelengths measured, which typically includes near-infrared, visible, and sometimes near-ultraviolet spectra. The use of dark-field imaging enhances the effectiveness of the technique since it decreases the background signal and emphasizes materials that scatter the most light, and such scattering spectra are more uniquely characteristic of a given material.[2–5]

Other early uses of HSI focused on long-range, large-scale applications for geologically oriented agencies, including surveyors, mineral, and oil industries. While previous forms of correlating spectroscopic and photographic data existed, narrow bands of collection meant the techniques were only suitable for certain compounds. The introduction of HSI significantly broadened the potential number of materials the system could identify and locate, including, but not limited to, clays, sulfates, carbonates, oxides, and silica, which had been otherwise impossible before.[6] HSI conducted from instruments mounted on orbiting satellites has provided a wealth of data for analysis for these industries.

The flexibility of HSI meant it also became a mainstay of other forms of surveying and large-scale analysis. It proved able to distinguish things such as water levels, flooding, plant populations, and indicators of health.[7] It was also an excellent tool for coordinating all the material information with mapping data. However, the technique did not remain solely in the hands of large-scale surveyors. The food industries have seen tremendous benefit from this technology, employing it as a screening tool. The detail of information, combined with its mapping format, enables quick assessment of issues such as batch-to-batch consistency, ripeness, defects, or contamination.[5] Yet for many years, the focus of this technology has been on large-scale questions. Only recently have the ideal optics been developed to translate the technology down to the nanoscale.

By comparison, conventional imaging techniques such as red/green/blue (RGB) imaging lacked spectral information whereas near-infrared (NIR) spectroscopy was unable to provide spatial information. Multispectral imaging was a leap forward from the conventional techniques, however, still had limitations. These challenges were overcome with HSI, as shown in Table 1.

HYPERSPECTRAL IMAGING TOOLS

One example of a relatively new tool with this capability at the nanoscale is the CytoViva® nanoscale microscope and HSI system (Auburn, Alabama, USA). Mounted on an Olympus BX-41 optical microscope (Melville, New York, USA), it employs a novel dark-field-based illuminator that focuses a highly collimated light at oblique angles on the sample. Resulting images have better contrast and higher signal-to-noise ratio when compared to images obtained via conventional dark-field microscopy. This is achieved by using the intrinsic light scattering properties of objects, materials, and biologicals so that prior staining of the sample is not necessary

TABLE 1 | Comparison of RGB Imaging, NIR Spectroscopy (NIRS), Multispectral Imaging (MSI) and Hyperspectral Imaging (HSI) (Reprinted with permission from Ref 5. Copyright 2007 Elsevier)

Feature	RGB Imaging	NIRS	MSI	HSI
Spatial information	√		√	√
Spectral information		√	Limited	√
Multi-constituent information	Limited	√	Limited	√
Sensitivity to minor components			Limited	√

Advantages and limitations of imaging modalities.

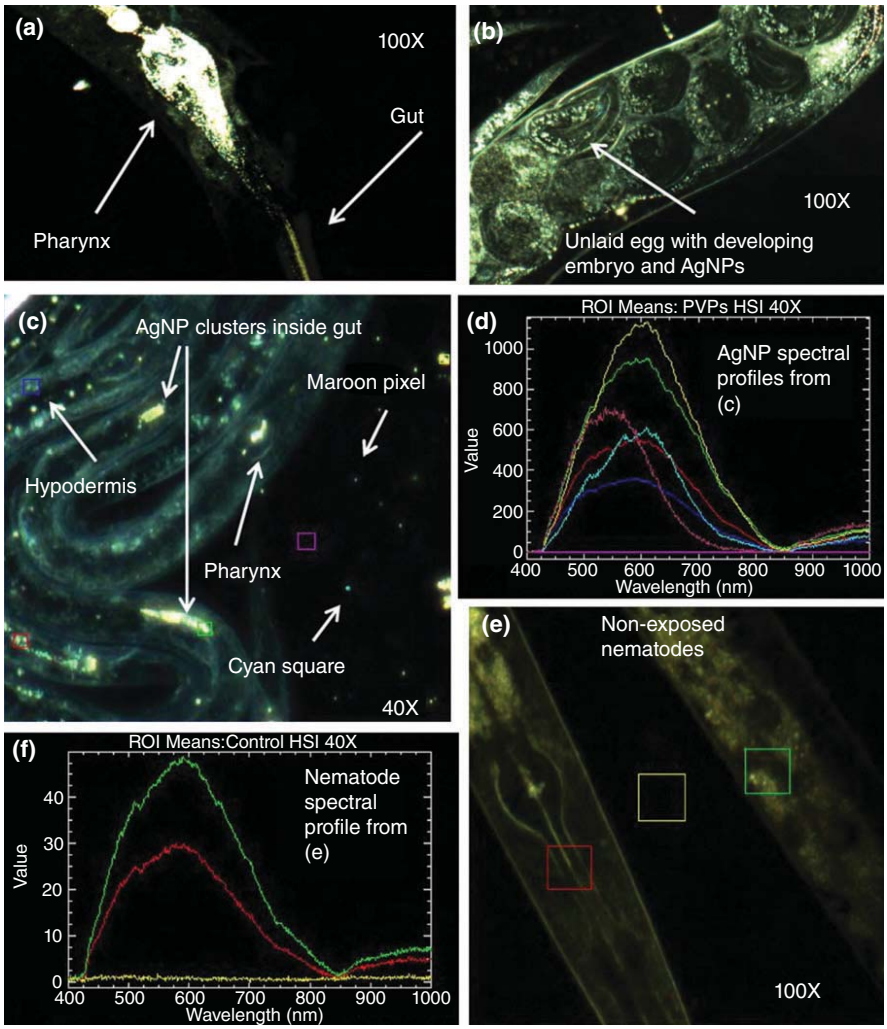

FIGURE 1 | Example of CytoViva® application for visualization of nanoparticle internalization into the cells of *Caenorhabditis elegans*. AgNPs are ingested and internalized into the cells of *C. elegans*. (a) CIT_{10} AgNPs are taken up along with food by *C. elegans*. (b) Some CIT_{10} AgNPs are also taken up into the cells of the nematodes, and are transferred to the offspring. AgNP identity was confirmed by hyperspectral analysis. (c) Hyperspectral image (HSI) showing the presences of PVP_S AgNPs inside and outside *C. elegans* after exposure; colored rectangles correspond to the pixel areas [regions of interest (ROI)] in HSI where spectral profiles are collected. (d) The spectral profiles of AgNPs and hypodermis region of *C. elegans*; green, red, and dark blue represent internal AgNPs clusters, yellow, cyan, and maroon external AgNP clusters, and magenta background. (e and f) Very little signal is detected in nonexposed nematodes; note that *y*-axis values are much lower in (f) than (d); higher contrast was used in (e) than (c) for visualization. Images taken using CytoViva hyperspectral imaging technology with dark-field microscopy at 100× (panels a, b and e) or 40× (panel c) total magnification. The color of spectral profile corresponds to color of the rectangle in the image and each profile represents the average of all the pixels present in each square. (Reprinted with permission from Ref 8. Copyright 2010 Elsevier)

for visualization. Spectral information about the sample can be obtained upon resolution of both the visible and near-infrared wavelengths (VNIR; 400–1000 nm) of scattered light with the HSI system and the Environment for Visualization software (ENVI 4.4 version).[8] The dark-field HSI system analyzes particles in solution or other matrices in such a way that it ignores artifacts that could lead to imprecise particle sizing if other advanced techniques, such as electron microscopy (EM), were used instead.[9,10] An example of images and spectral profiles that can be obtained with CytoViva is shown in Figure 1.

There are several additional HSI tools currently in use for a variety of applications and analyses that are reporting nanoscale imaging capabilities. Resonon (Bozeman, MT) offers benchtop HSI systems that can be used not only for laboratory research but also for outdoor field analysis.[11] Its hyperspectral camera has a spectrometric range of 400–1700 nm. SPECIM, a Finland-based company, offers several cameras and scanners for HSI that are suitable for a variety of purposes, including laboratory-based research, industry, environmental, and defense applications.[12] Norsk Elektro Optikk (NEO; Lørenskog, Norway)

TABLE 2 | Features and Capabilities of Selected HSI Systems

HSI System	Spectral Range	Spectral Resolution	Spatial Resolution	Signal-to-Noise Ratio	Light Source	Imaging Software
Resonon[11]	350–1700 nm	2.1 nm	—	1935:1	Halogen	SpectrononPro
SPECIM[12]	400–1000 nm	2.8 nm	0.19 nm	600–1000:1	Varies by application	SpecSensor SDK
Norsk Elektro Optikk[13]	400–2500 nm	3.7 nm	—	—	LED	"dedicated software"
CytoViva[10]	400–1000 nm	2.0 nm	—	—	High power halogen	ENVI
P&P Optica[14]	350–2500 nm	0.1 nm	—	—	Halogen	PPO IRIS
Photon Etc.[15]	400–1000 nm	0.2 nm	—	—	Tunable laser	PHySpec
Surface Optics Corporation[16]	400–1000 nm	4.68 nm	—	—	Halogen	SRAnalysis
Gooch & Housego[17]	400–1000 nm	0.6 nm	—	—	halogen	μ-Manager
PARISS[19]	365–920 nm	1 nm	0.6 μm × 0.6 μm	—	Varies by application	PARISS

The features and capabilities of the HSI systems discussed in this review are summarized in Table 2. The product specifications were obtained from the vendors' websites and/or through direct communication with the vendors. Blanks (—) indicate information that was not available in the product information sheets. For these systems, the vendors indicate these parameters are variable based on the specific system and HSI camera as well as experimental design.

offers turnkey hyperspectral systems for laboratory, airborne, field, and industrial use, which incorporate one of NEO's line of HySpex cameras, each with a different range.[13] P&P Optica is an Ontario-based company that manufactures hyperspectral spectrophotometers, including the PPO HyperChannel, which can be coupled to imaging acquisition and analysis software.[14] Benchtop HSI systems are also available from Photon Etc. (Montreal, Quebec, Canada), whose imaging system is capable of selecting images with a 2 nm bandwidth from 400 nm to 1000 nm and is being used in nanotechnology-based research.[15] Another player in the HSI field is Surface Optics Corporation (San Diego, CA), which provides imaging systems with spectral ranges from ultraviolet through infrared, primarily for laboratory research applications.[16] The HSi-440C Hyperspectral Imaging System by Gooch & Housego (Orlando, FL) can image and analyze multiple signals in fixed and living cells at video rates.[17,18] Lastly, PARISS® (Prism and Reflector Imaging Spectroscopy System) Analytical Hyperspectral Imaging System can be used for the detection and analysis of metallic and nonmetallic NPs and is based upon a prism and reflector system.[19] The prism has several advantages, such as nearly 100% efficiency throughout the spectrum, higher sensitivity and zero diffraction over the diffraction grating system as compared to other similar systems.[19] Table 2 summarizes the features and capabilities of each HSI system discussed here.

IN VITRO APPLICATIONS

The difficulties of assessing nanomaterials in cells are compelling; currently, the only tool amenable to biological sample preparation and direct visualization of NPs is the electron microscope. Unfortunately, visualization by TEM and scanning electron microscopy (SEM) is an intensive process: analysis is slow and difficult to automate and nanomaterials may be present in such low quantities that they prove impossible to find. Worse still, sample preparation can sometimes disrupt nanomaterials (whose states are always precarious), resulting in artifacts that may give a false impression (e.g., the observation of large agglomerates which are formed by a wet sample drying, but are fundamentally indistinguishable from other agglomerates that were present in the sample in that state before preparation).

Hyperspectral microscopy as a complementary imaging technique provides a potential solution to some of these issues. An example is a study in which human macrophage cell lines (U937) exposed to silver nanoparticles (AgNPs) were fixed with formaldehyde and imaged directly on glass slides using hyperspectral microscopy. The microscope could successfully identify both intracellular and extracellular clusters of NPs and map them to locations of interest (see Figure 2).[20] Another study employed hyperspectral microscopy as a validation method in order to determine that their superparamagnetic iron oxide nanoparticles (SPIONs) were successfully linked to the targeted cells. Mapping could distinguish the NPs and demonstrated this correspondence, which is intended to be used in a later labeling application.[21] Another study focused on the potential of synergistic toxic effects between carbon nanotubes (CNTs) and herbicides on photosynthetic algae, and utilized hyperspectral microscopy as a method to locate CNTs in solution. CNTs could be clearly identified in clusters around the algae, providing additional information regarding interactions that may not have been otherwise apparent.[22]

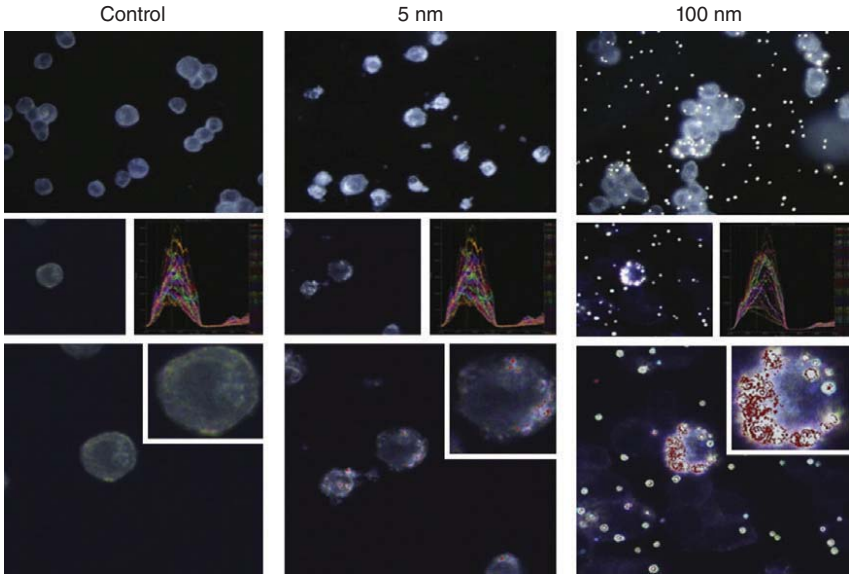

FIGURE 2 | Visualization of intra- and extracellular clusters of nanoparticles. Internalization of silver nanoparticles in U937 cells was examined with CytoViva URI system 2 h after silver nanoparticles treatment (2.5 μg/mL). Silver nanoparticles of 100 nm were detected inside the cells and presented as multiple red spots. With 5 nm silver nanoparticles treatment, several red spots suggested internalization of 5 nm silver nanoparticles, which was not detected in the control. (Reprinted with permission from Ref 20. Copyright 2012 Elsevier)

Enhanced dark-field microscopy (EDFM) can also be used to visualize cellular interactions with NPs, including cellular uptake. One study assessed the effects of gold and silver NPs on human keratinocyte (HaCaT) and rat adrenal gland (PC-12) cells and observed cellular uptake of these NPs via CytoViva HSI. Cellular NP uptake was confirmed by TEM.[23] Another study was designed to investigate cellular interactions of AgNPs (Ag-15 nm, Ag-30 nm, and Ag-55 nm) with rat alveolar macrophages for their potential role in initiating oxidative stress and inflammatory and immune responses. Hyperspectral images showed brightly illuminated areas in the microphages, suggesting uptake of silver NPs and agglomerates inside the cells. This was likewise confirmed by TEM analysis.[24] Similarly, another study utilized the EDFM capabilities of CytoViva to monitor uptake of aromatic thiol-modified gold nanoparticles (AuNPs) in a human lung carcinoma cell line (A549).[25]

Hyperspectral microscopy has proven to be a good tool for not only visualizing cellular uptake and binding of NPs, but also for simultaneous compositional identification of those same NPs *in vitro*. Santos et al.[26] demonstrated the uptake of retinoic acid $(RA)^+$-NPs by neural stem cells of the subventricular zone (SVZ) and matched their spectral profiles to a reference spectral library, created by acquiring spectral profiles of $(RA)^+$-NPs in an aqueous suspension, thereby confirming the identity of the NPs observed.

The CytoViva imaging system can allow for relative determination of the size of NPs in solution through observation of Brownian motion: Chumakova et al.[27] estimated the sizes of suspended NPs based on the intensity of the Brownian motion in real time (see Figure 3). The Brownian motion of the NPs resulted in gray traces around the particles. The size of these gray traces was inversely proportional to the size and weight of the NPs: smaller, lighter NPs move faster in solution and thus create larger 'spots.' While this is not a quantitative method, it does allow for an indirect assessment and relative estimation of particle size. Others have utilized this system to visualize and characterize NPs in solution prior to using the NPs in experimental exposure models.[28]

It is evident from the literature that hyperspectral microscopy is capable of finding and identifying many different types of nanomaterials. Moreover, it is faster and less expensive than EM. While it may not be able to provide the precise sizing information that an EM measurement would, it certainly provides a valid tool for determining the location of nanomaterials in a system as well as for detecting them in order to then justify further investigation using more intensive methods.

IN VIVO APPLICATIONS

The challenges for *in vivo* analysis of nanomaterials resemble those of *in vitro*, but with additional complications. The largest complication arises from the potential for nanomaterials to translocate to distant organs in the body, either by passing directly through membranes or by uptake into circulatory or other systems. This makes it difficult or impossible to accurately predict in which organs nanomaterial will concentrate since they may not remain at the initial site of exposure. Additionally, if nanomaterials preferentially localize to specific structures in a particular organ, it is possible to section an organ for imaging

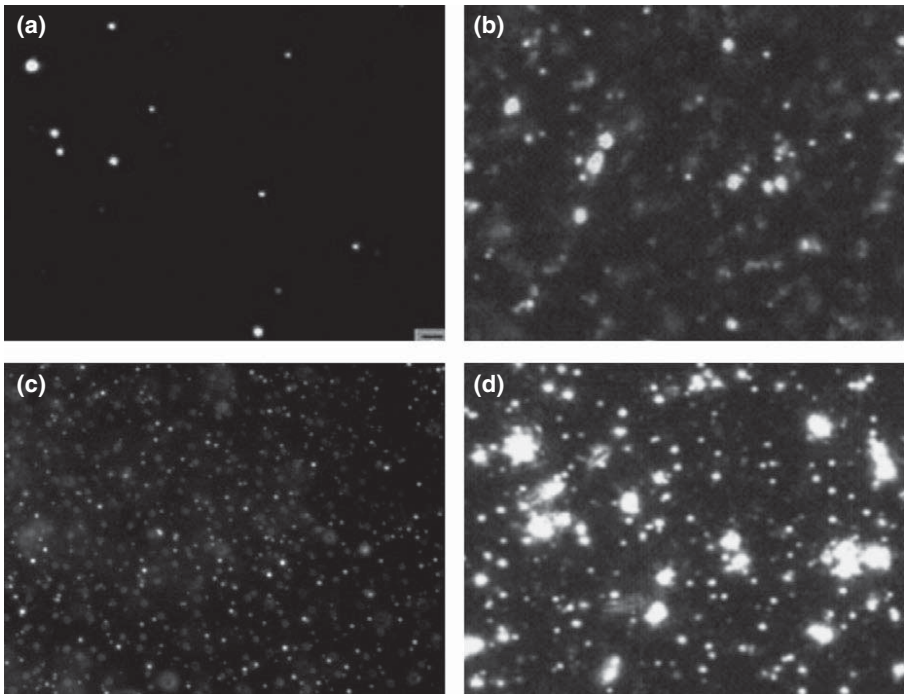

FIGURE 3 | Visualization of nanoparticles in suspension. Light scattering images of the nanoparticle suspensions obtained by Olympus microscope BX51 with the *CytoViva* Adapter (100x oil objective): (a) 5% glucose, (b) PLGA, (c) PEI/DNA, and (d) complex PLGA/PEI/DNA. Bar = 5 μm. (Reprinted with permission from Ref 27. Copyright 2008 Elsevier)

and fail to locate the nanomaterials. This is especially difficult for TEM due to the sample cross-section thickness of a few hundred nanometers. Thus, there is need for a solution that would eliminate or improve the efficiency of EM analysis.

Two direct demonstrations of HSI *in vivo* include a pair of studies on the uptake of ingested silver. In one, Japanese medaka in a silver nanoparticle-containing environment were examined, and the researchers were able to definitively show that the silver was not only in lung tissues but also found in brain, eye, gill, and gut tissues.[29] The second study was similar, in which the hyperspectral microscope was successfully employed to locate silver NPs in nematodes after ingestion.[8] Similar to these studies, Kim et al.[30] used HSI to assess the interactions of citrate-coated AgNPs with the surfaces of nematodes. Another study employed similar techniques to examine the fate of gold NPs injected into the nervous system of a cockroach and their clearing time.[31]

The same advantages have also been demonstrated in the analysis of mammalian tissues. One mouse study demonstrated the time-dependent relationship of titanium dioxide NP burden in the lung following intratracheal installation. This indicates that the technique is not merely capable of locating materials of interest (see Figure 4, which also demonstrates the effectiveness of spectral mapping) but is also capable of estimating relative levels those materials.[32] In a similar study, intratracheal installation of ceria NPs into rats was examined, and particles were easily identifiable in both specific lung cells and pulmonary fibroblasts, as indicated in Figure 5.[33] Another mouse study demonstrates a similar, semi-quantitative approach to measuring the gradual biological degradation of CNTs in lung tissues.[34] Another investigation of CNT degradation employed enhanced dark-field imaging to demonstrate that the majority of inhaled CNTs remain in the alveoli or are taken up by resident macrophages, and the biochemical action of those macrophages likely plays a role in associated pathology as well as nanotube degradation.[35] Visualization of MWCNT localization was demonstrated in several studies, such as an examination of lung tissues following a 56-day *in vivo* rat exposure.[36] Further demonstrating the utility of this technique, HSI was employed to demonstrate systemic transport of multi-walled carbon nanotubes (MWCNTs) from the lungs to the liver, kidneys, and heart of rats exposed via inhalation or intratracheal instillation. Furthermore, the system was utilized to generate MWCNT counts for each tissue examined.[37]

HSI has also shown utility for studying NP interactions with viruses and other biological targets: HSI was used to visualize fullerenes and viruses in a study of bacteriophage and $^1O_2$ generation inactivation

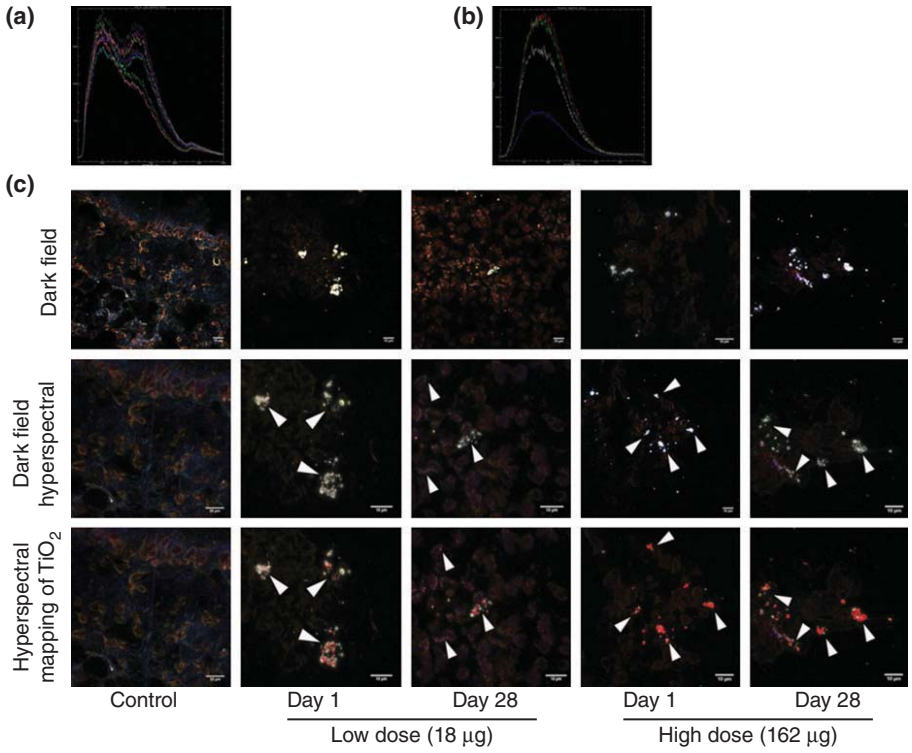

FIGURE 4 | Identification of nano-TiO_2 particles in lung tissues. Lung tissues from mice harvested 1 and 28 days following a single intratracheal instillation of low (18 μg) and high (162 μg) doses of nano-TiO_2 were subjected to VNIR hyperspectral imaging to identify particle retention in these tissues. (a) Reference spectral library from nano-TiO_2 exposed tissue. (b) Reference spectral library from control tissue. (c) Dark-field images from nano-TiO_2 exposed tissues (upper panel). Dark-field hyperspectral images from nano-TiO_2 exposed tissues identifying these nanoparticles, which appeared as aggregates of white inclusions (middle panel). Hyperspectral mapping of nano-TiO_2 in these tissues appeared as red dots or aggregates (bottom panel). (Reprinted with permission from Ref 32. Copyright 2013 Elsevier)

rates and surface functionalization-dependent antiviral properties of fullerenes.[38]

These examples serve to demonstrate that hyperspectral microscopy may be useful for both *in vivo* and *in vitro* studies. It can provide relative quantitation of materials, detailed localization of nanomaterials, and is capable of analyzing a wide range of potential analytes from noble metals, to metallic oxides, to carbon nanotubes. This flexibility will certainly reduce the need for EM and, in some cases, may eliminate it entirely.

TOXICITY STUDIES

The HSI system is also useful for assessing toxic effects of nanomaterials, including cellular uptake and viability, as well as systemic transport. It has been used to evaluate possible morphological changes induced by single-walled carbon nanotubes (SWCNT) or SWCNT-PEG (polyethylene glycol) in cell culture. A study in which PC-12 cells were incubated with either SWCNTs or SWCNT-PEGs suggested the SWCNTs appeared to be more toxic to PC-12 cells than the SWCNT-PEGs. These results supported earlier reports indicating that surface modification plays a role in NP cellular uptake, bioactivity, and possible toxic effects. EDFM enables the examination of surface functionalization of these nanomaterials and their biological interaction with cellular systems.[39]

Cellular internalization of nanoscale materials *in vitro* was also studied by Grabinski et al.[40] who employed an EDFM system to observe uptake of various functionalized gold nanorods (GNRs) in a human keratinocyte cell line (HaCaT) and subsequent changes in cellular morphology. TEM analysis confirmed GNR internalization. DeBrosse et al.[41] conducted a similar study in which they used fluorescence microscopy to examine the interface between HaCaT cells and GNRs. The images they obtained showed strong cellular interactions with the GNRs as well as the presence of GNR agglomerates.

In a study testing how various NP compositions, shapes, and coatings affect microglia (immune cells residing in the brain), HSI analysis was used to monitor particle uptake. It was demonstrated that cetyl trimethylammonium bromide (CTAB)-coated GNRs

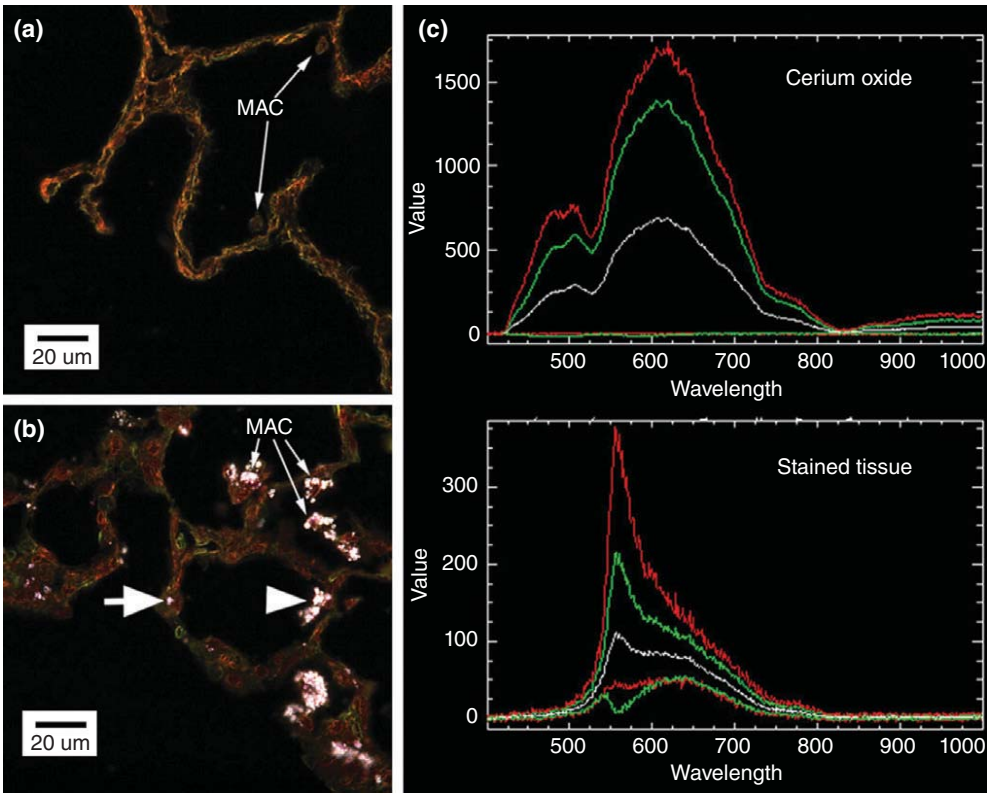

FIGURE 5 | Cerium oxide particles in lung tissue and pulmonary fibroblasts isolated from CeO_2-exposed rats, at 28 days post-exposure. Cerium oxide particles in lung tissue and pulmonary fibroblasts isolated from CeO_2 (a single intratracheal dose of 7 mg/kg)-exposed rats, at 28 days post-exposure. Control lung tissues exhibit no particles under high resolution, dark-field illumination (a). Illuminated CeO_2 particles, using dark-field-based illumination, were clearly detected in macrophages (MAC), the interstitium (arrow), in acellular surfactant clumps (arrow head), in the airspace as free particles (b). (c) Representative intensity versus wavelength spectra of points (pixels) of CeO_2 particles in the cerium oxide-exposed tissue section (upper panel) and spectra of control tissue. Each different colored curve represents a different point. Small arrow: MAC; big arrow: interstitium; arrow head: acellular mass of surfactant-cerium oxide in the air space. (Reprinted with permission from Ref 33. Copyright 2012 Elsevier)

and PEG-coated urchins were taken up by microglial cells without loss of viability. Furthermore, based on the HSI analysis, the extent of internalization of gold NPs appeared to be shape-dependent.[42]

An examination of the distribution and clearing of NPs by rats used dark-field illumination to show the presence of fluorescently loaded NPs (20 nm, 100 nm, or 1000 nm latex fluorospheres) in tissue homogenates. They were able to not only demonstrate significant agglomeration, but also demonstrate that the liver, spleen, and lung were the greatest repositories for all NPs following intravenous injection. The lung was found to be the greatest repository for fluorospheres of all sizes following either single or multiple airway exposure (Figure 6).[43]

A study investigating the toxic effects of tetrahydrofuran (THF) and C_{60} NP aggregates on zebrafish survival, behavior, and gene expression employed the EDFM system to study the aggregation of C_{60} particles, demonstrating their propensity to form aggregates up to three-times the size of the original latex NPs of 100 nm. The use of the HSI system allowed the researchers to avoid artifacts that might arise from preparation of TEM samples, such as the possibility of altering particle size or altering their level of agglomeration.[44]

CLINICAL APPLICATIONS

There are additional promising applications aimed at the development of medical diagnostics and therapeutics. Such a technique would be useful for examining nanomaterial fabrication, encapsulation, and similar processes, particularly when other analyses might risk damaging fragile constructs. In one case, the colocalization of a mesoporous-silicon-encapsulated chemotherapeutic drug to the target organ was validated by hyperspectral microscopy.[45] Another diagnostic technique applied the technology in a similar way: using hyperspectral microscopy as a means to

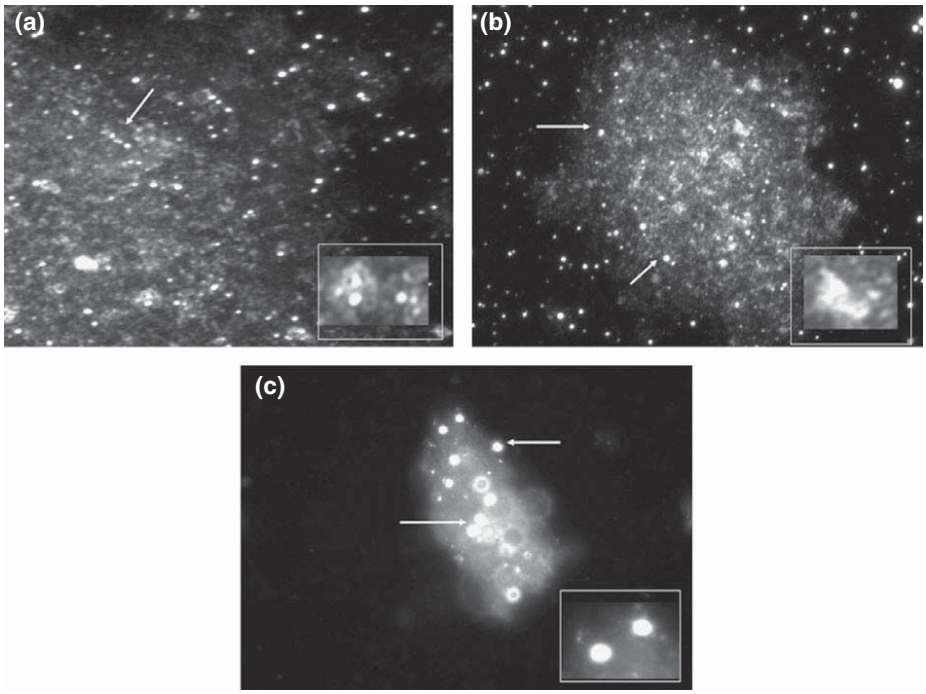

FIGURE 6 | Dark-field imaging of nanospheres in lung homogenates. (a–c) Polystyrene spheres in lung homogenates (1 day post-exposure) imaged by dark-field illumination (CytoViva). A sample of homogenate was allowed to dry on a slide. The lung tissue had a dull and spotty reflective property while the spheres generate very bright, spherical images. There is a clear difference between the 1000 nm spheres (c) versus the 100 nm (b) and 20 nm (a) spheres. The inserts show magnified areas of the spheres in tissue; some agglomeration of 20 nm and 100 nm spheres can be seen but the 1000 nm spheres appear to be monodisperse. Owing to the resolution of the microscope there is no difference in the image of the 20 nm spheres versus the 100 nm spheres. Arrows point to the spheres. (Reprinted with permission from Ref 43. Copyright 2009 Elsevier)

quantify the difference of scattering in tissues targeted by the immuno-gold NP label.[46]

The technique is also amenable to characterization of single NPs and their interactions with or in the presence of corresponding biomolecules. The reflectance spectra of a material at the nanoscale is dependent not only on the material properties but on its electrical properties, including surface plasmon resonance. These effects can vary significantly for differing locations on nonspherical particles or in the presence of a microenvironment that affects those electrical properties and, in conjunction with a proper excitation source and high-resolution detector, HSI may be used to note spectral changes indicating differences in orientation or interactions in single particles.[47] In such a way, HSI may enable detection of trace amounts of specific ionic or molecular analytes depending on their interactions with select, well-characterized NPs.

In clinical applications, use of hyperspectral microscopy has been employed to visualize and identify microscale materials as well as nanoscale materials. A clinically relevant *in vitro* study investigated the use of monitoring well-characterized microparticles (those greater than 1000 nm) in the circulatory system as a measure of propensity to premature coronary calcification by employing a dual-mode fluorescence and optical microscopy system in the analysis of freshly isolated blood-borne, calcified microparticles.[48]

A study employed single molecule imaging in an *in vivo* cell signaling by using signature NP clusters to effectively label biomolecules of interest (in this case, proteins) for HSI and spectroscopy. This enabled *in vitro* visualization of the molecules during discrete enzymatic steps. The change in intensity and color of scattering light was studied and indicated the trajectories of the single molecule in live cells.[49]

Another study employed time-dependent HSI of AgNP uptake by bacterial cells. Uptake was found to increase with incubation time. Also, the individual NPs and single bacterial cell spectra were recorded using HSI system. This is another good example of using HSI to monitor single cell interactions with NPs.[50]

A group investigating the antimicrobial properties of NPs based on their interactions with *Candida albicans* was frustrated in their attempts to employ SEM by preparation artifacts leading to improper observations of NP-*Candida* surface interactions. The researchers then used an EDFM system

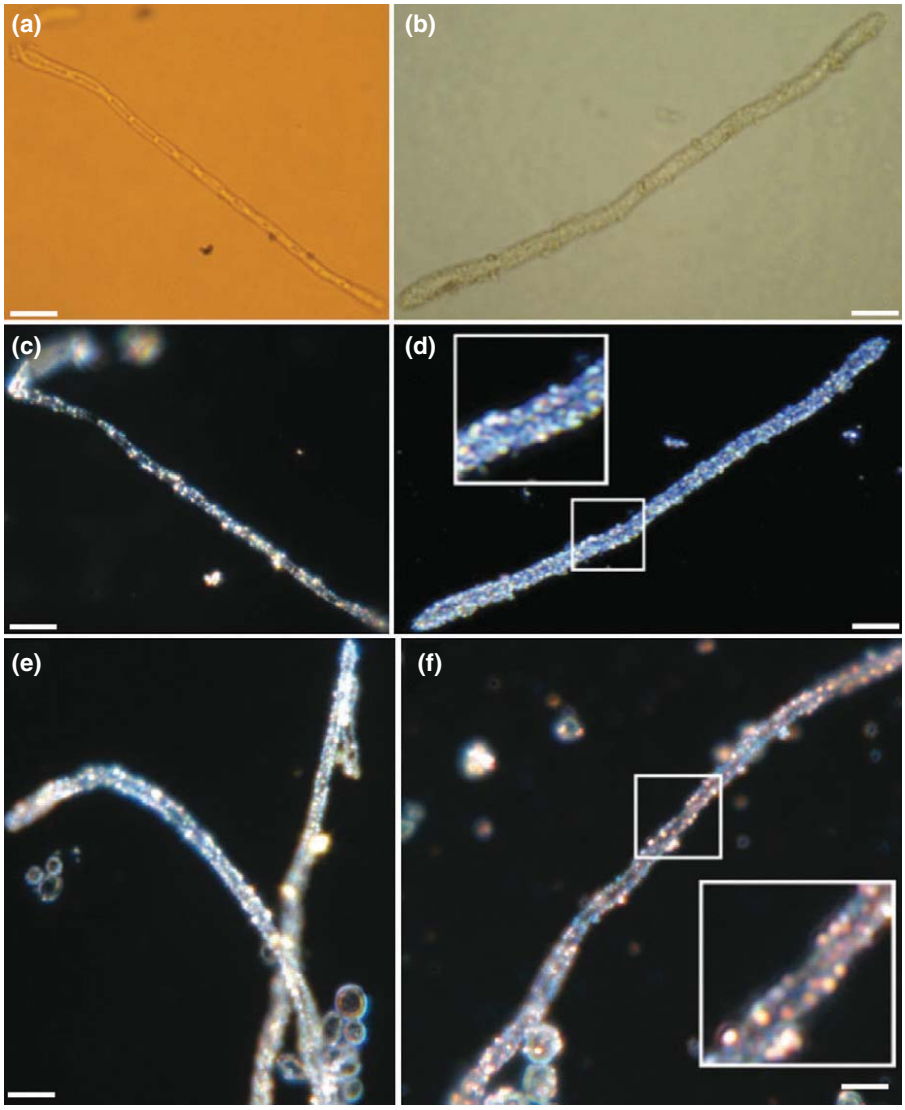

FIGURE 7 | Comparison of nanoparticle binding via light and enhanced dark field microscopies. (a) Silver NP (MIC of 31.25 ppm) viewed via light microscopy (bound NP not detectable). (c) Silver NP viewed via dark-field microscopy (NP easily detected). (b) Cobalt NPs (MIC of 0.24 ppm) viewed via light microscopy (encrustation of cobalt NP visible even via light microscopy). (d) Binding of cobalt NP viewed via enhanced dark-field microscopy. Inset shows detail of highlighted area, magnified 2.25×. (e) Copper NP (MIC of 15.63 ppm) demonstrating 'bejeweled' appearance. Inset shows detail of highlighted area, magnified 2.5×. (f) 'Bejeweled' appearance of copper–silver alloy NP (MIC of 250 ppm). Scale bars for all panels 5 μm. (Reprinted with permission from Ref 48. Copyright 2009 Elsevier)

as an alternative instrument with success, suggesting implications for using this system for screening NP antimicrobial properties based on visualization of their interactions with cell surfaces (see Figure 7).[51]

Another example is the development of a tumor-labeling approach using micelle-encapsulated SPIONs. Hyperspectral microscopy was able to differentiate both the makeup of the vesicles and the NPs, and to show the presence of NP cores to vesicle rings.[28] A related application is the use of hyperspectral microscopy as a method to roughly quantitate particle abundance and the size of agglomerates, a method that is particularly useful for mixed-materials samples which typically cause light scattering techniques to fail; this method was demonstrated in a two-micelle system.[52]

In a cell targeting study conducted by Jayanna et al.[53] fluorescently stained mixtures of human bone metastasis-derived prostatic adenocarcinoma (PC3) and human embryonic kidney (HEK293) cells treated with liposomes were visualized with HSI using fluorescent filters to determine the extent and location of liposome binding. They demonstrated enhanced cytotoxic effects of liposomes that were loaded with

doxorubicin against PC3 cells, suggesting a potential mechanism for targeted therapeutics in the treatment of prostate tumors.

Enhanced dark-field and HSI were employed to visualize uptake of AgNPs with and without surface functionalization in the presence or absence of natural organic matter (NOM) in *Caenorhabditis elegans*.[54] Hyperspectral mapping confirmed gut uptake of citrate-functionalized AgNPs and identified AgNP-NOM interaction, which was shown to rescue exposure-induced cellular damage. [54]

Another study demonstrating the strength of EDFM and HSI to locate and characterize NP involved examining nanoceria in living *C. elegans*. In this case, dark-field imaging was used to find particles ingested by nematodes and then spectral mapping helped to further distinguish the ingested ceria.[55]

The technique also found utility in the development of therapeutic chemicals that act on NP dispersion. Wang et al.[56] studied the effect of Survanta® (North Chicago, Illinois, USA) *in vivo* and *in vitro* on SWCNT dispersion compared to previously studied sonication and acetone methods. The hyperspectral images of dispersed and nondispersed SWCNT yielded clear visualization of the effects of the surfactant, demonstrating the usefulness of HSI as a quick screening tool to study dispersions.

ENVIRONMENTAL APPLICATIONS

Environmental samples are difficult to characterize owing primarily to two traits: enormous variation in potential matrices in which they are collected (air, water, soil, etc.) and significant heterogeneity between samples (leading to high variance within in a set of samples). The addition of nanoparticulates further complicates analysis due to their unique properties, which often include a propensity to agglomerate and adhere to surfaces in complex matrices. Any sample preparation that significantly modifies the matrix may significantly alter the state of nanomaterials in the system. Furthermore, EM may not be able to provide enough specificity or contrast for adequate visualization of nanomaterials in environmental matrices.[57] Consequently, a system that offers high-contrast visualization and is both adaptable and requires minimal sample modification is ideal for environmental sampling.

Use of HSI for nanoscale environmental applications is in its infancy, but shows great promise in tackling complex samples. A method was developed to use hyperspectral microscopy to examine environmental water samples. In this case, simulated wetland ecosystem water was spiked with NPs, including Ag, TiO_2, CeO_2, C_{60}, and CNTs (both single- and multi-walled as well as unmodified and carboxylated). Small volumes of sample were dried on a slide and spread as they dried to minimize agglomeration. From these samples, NPs could be distinguished, relative levels established, locations mapped, and even differentiated in terms of whether particles of the same core compound were coated or not (see Figure 8).[58]

A recent study tested an affordable filter-based drinking water purification system that releases a constant flow of silver ions into the water. HSI was used to study the fate of NPs in this system by checking for sustained release of silver ions into the water and to confirm the antimicrobial activity of the silver NP-coated aluminum oxyhydroxide-chitosan composite.[59]

HSI has also been employed to study NP formation and interaction with bacteria in real-time model environmental systems. One study used the system to investigate different properties of the matrix and their effects on silver-particle nucleation and growth, as well as to study their interactions with *Pseudomonas aeruginosa*, enabling investigation of the very mechanisms pertaining to NP generation and stability in a complex matrix.[60] While this area has not yet been thoroughly explored, this paper, in conjunction with the established history of HSI being a tool for geological investigation, indicates hyperspectral microscopy could be a promising technology for environmental detection of NPs, especially those comprised of uncommon or engineered materials.

LIMITATIONS

Hyperspectral microscopy is not without limitations arising from its light-based mode of operation. Foremost, its spatial resolution is not great enough to differentiate individual particles from their agglomerates, and thus it is not likely to be able to differentiate the two, which may limit its use for *in vitro* toxicology studies or in examination of agglomeration potential in fluid matrices. Attempting to differentiate differently sized particles will need to take the form of quantifying either the change in illumination or spectral profile of a few pixels, and as the response will differ significantly by material, it may complicate the analysis if the size of agglomerates to be studied varies significantly.

Additionally, the technique is highly dependent on the material of interest. While in theory any material will have a characteristic spectral profile, reflectance spectra of some materials are more easily detected and characterized than others. Specifically, the spectral profile is a question of surface plasmon

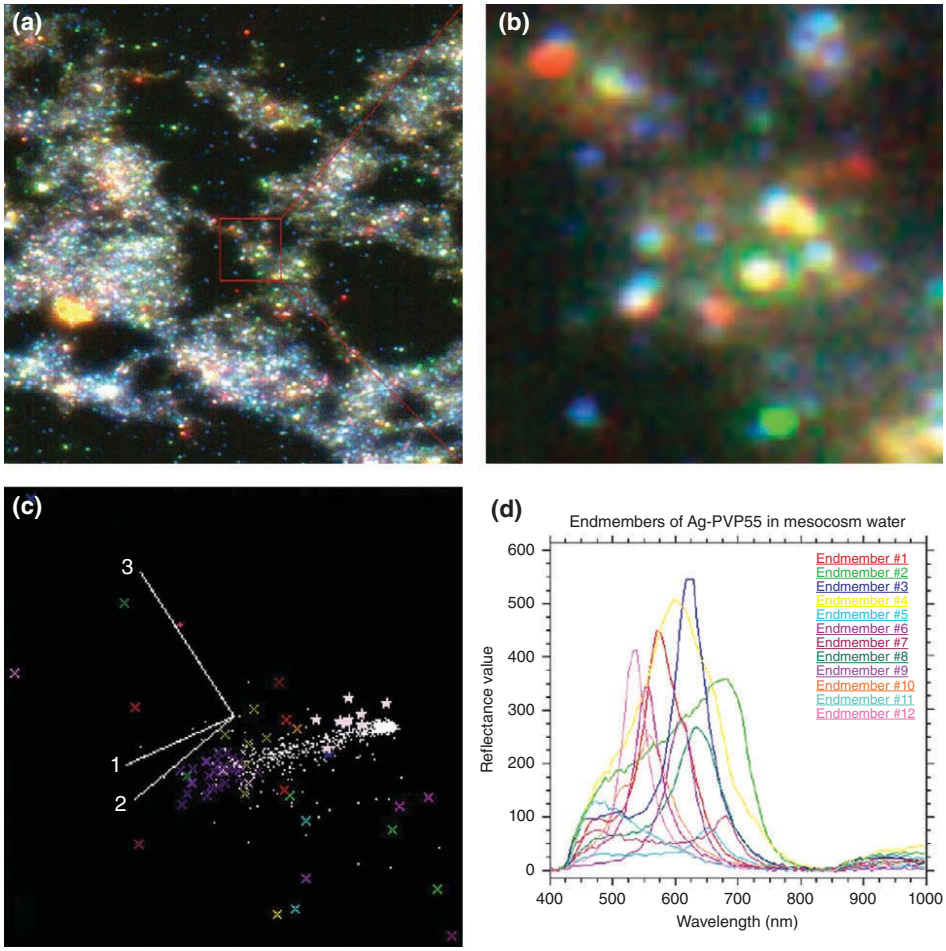

FIGURE 8 | Hyperspectral imaging of nanoparticles in complex waters. Hyperspectral image of Ag-PVP_{55} nanoparticles in mesocosm (a), 600× zoom in of a portion of the sample image (a), (c) n-dimensional visualization analysis of endmembers, and (d) endmembers of Ag-PVP_{55} nanoparticles of different sizes the sample. Images were acquired using 100× objective/1.3 oil iris. Scale: 2 cm = 200 μm. (Reprinted with permission from Ref 58. Copyright 2012 Elsevier)

resonance, which is why noble metals such as silver and gold figure prominently. Other metallic materials can also be well-characterized. However, characterizations of semi-metallic or organic materials may prove more difficult. This is amplified by the difficulty of selection for reference spectra, as for NPs, the parameters that produce them will vary significantly depending on their microenvironment. This can be advantageous or disadvantageous for a particular study, but will always complicate analysis.

More significantly is that while it enables the detection of nanomaterials, no study has precisely quantified the rate of false-positive identification or assessed its efficacy in the presence of stains used in histology or immunohistochemistry. The technique is also sufficiently novel that there are few standardized methods to be applied, with the result that each lab may use differing source power, exposure time, or other parameters which can result in significant variance in spectra of similar materials analyzed under different conditions. However, if hyperspectral microscopy is treated as a screening tool or a method of spatial location rather than a final quantification method, it will still be significantly advantageous both to research as well as biological sample analysis. Moreover, as it gains more acceptance in medical or research laboratories, it is likely that reference spectral libraries designed for specified conditions will emerge which will make it easier to apply the technique to larger numbers of varied sample materials.

CONCLUSIONS

Despite its obvious promise, hyperspectral microscopy is still a relatively new technology that has yet to carve out its own niche or to enter those dominated by current technologies. One area where this technology is also being explored is for histological analyses, where

it is uniquely suited to identify unlabeled nanomaterials in tissue samples. Removing the need for labeling is also advantageous in cellular biology, where labeling may affect the NPs' properties and the experiment results. Hyperspectral microscopy allows for investigation of materials in a more native state and truer to conditions of biomedical relevance, which would also benefit the emerging study of nanotoxicology where mechanisms of action are still poorly understood.

Additionally, while some studies have applied hyperspectral microscopy to the analysis of environmental samples, there is clearly room for further exploration in this field. Analysis of soil by this method has obvious potential as the technique itself found its earliest macroscopic applications in geologic surveying. However, analysis of air or water samples is hindered by the challenge of immobilizing particles for analysis and generating relevant standards against which to measure. Refinement of methods for analyzing air and water samples is of great interest, not only to environmental biologists and toxicologists, but also to corporate entities who, as nanomaterials become increasingly scrutinized, will desire less costly methods of testing for these materials than the current standard: electron microscopy.

ACKNOWLEDGMENTS

The manuscript was written through contributions of all authors. G.A. Roth and S. Tahiliani contributed equally. All authors have given approval to the final version of the manuscript. This work was supported by CDC-NIOSH grant OH-009990-01A1 and the NanoHealth and Safety Center, New York State, awarded to S. Brenner.

REFERENCES

1. Manolakis D, Marden D, Shaw GA. Hyperspectral image processing for automatic target detection applications. *Lincoln Lab J* 2003, 14:79–116.
2. Egan CK, Jacques SDM, Connolley T, Wilson MD, Veale MC, Seller P, Cernik RJ. Dark-field hyperspectral X-ray imaging. Royal Society Publishing. Available at: http://royalsocietypublishing.org/content/royprsa/470/2165/20130629.full.pdf. Accessed October 2014.
3. Photon Etc. Darkfield hyperspectral imaging for analysis of nanoparticles in cancer cells. Available at: http://www.news-medical.net/whitepaper/20140122/Darkfield-Hyperspectral-Imaging-for-Analysis-of-Nanoparticles-in-Cancer-Cells.aspx. (Accessed October 2014).
4. MicroImages. Introduction to hyperspectral imaging. Available at: http://www.microimages.com/documentation/Tutorials/hyprspec.pdf. (Accessed October 2014).
5. Gowen A, O'Donnell C, Cullen P, Downey G, Frias J. Hyperspectral imaging – an emerging process analytical tool for food quality and safety control. *Trends Food Sci Technol* 2007, 18:590–598.
6. van der Meer FD, van der Werff HMA, van Ruitenbeek FJA, Hecker CA, Bakker WH, Noomen MF, van der Meijde M, Carranza EJM, de Smeth JB, Twoldai T. Multi- and hyperspectral geologic remote sensing: a review. *Int J Appl Earth Obs Geoinform* 2012, 14:112–128.
7. Govender M, Chetty K, Bulcock H. A review of hyperspectral remote sensing and its application in vegetation and water resource studies. *Water SA* 2007, 33:145–151.
8. Meyer JN, Lord CA, Yang XY, Turner EA, Badireddy AR, Marinakos SM, Chilkoti A, Wiesner MR, Auffan M. Intracellular uptake and associated toxicity of silver nanoparticles in *Caenorhabditis elegans*. *Aquat Toxicol* 2010, 100:140–150.
9. Vetten MA, Tlotleng N, Rascher DT, Skepu A, Keter FK, Boodhia K, Koekemoer LA, Andraos C, Tshikhudo R, Gulumian M. Label-free *in vitro* toxicity and uptake assessment of citrate stabilised gold nanoparticles in three cell lines. *Part Fibre Toxicol* 2013, 10.
10. CytoViva. Hyperspectral microscopy: visible near infrared (VNIR) and short wave infrared (SWIR). Available at: http://www.cytoviva.com/products/hyperspectral-imaging-2/hyperspectral-imaging/. (Accessed January 2014).
11. Resonon. Benchtop hyperspectral imaging systems. Available at: http://www.resonon.com/products_benchtop_systems.html. (Accessed February 2014).
12. Specim. Hyperspectral imaging cameras and systems. Available at: http://www.specim.fi. (Accessed February 2014).
13. HySpex. Norsk Elektro Optikk. Available at: http://www.hyspex.no/index.php. (Accessed February 2014).
14. P&P Optica. Available at: http://www.ppo.ca/home. (Accessed February 2014).
15. Photon Etc. Hyperspectral imaging and spectroscopy instruments and applications. Available at: http://www.photonetc.com/index.php. (Accessed February 2014).
16. Surface Optics Corp. Hyperspectral and multispectral imagers. Available at: http://surfaceoptics.

com/products/hyperspectral-imaging/. (Accessed February 2014).

17. Gooch & Housego. Instrumentation. Available at: http://goochandhousego.com/product-categories/instrumentation/. (Accessed February 2014).
18. Leavesley SJ, Annamdevula N, Boni J, Stocker S, Grant K, Troyanovsky B, Rich TC, Alvarez DF. Hyperspectral imaging microscopy for identification and quantitative analysis of fluorescently-labeled cells in highly autofluorescent tissue. *J Biophoton* 2012, 5:67–84.
19. PARISS®. Nanoparticle analysis using the PARISS® analytical hyperspectral imaging system. Available at: http://www.nanoparticleanalysis.com/index.html. (Accessed October 2014).
20. Lim DH, Jang J, Kim S, Kang T, Lee K, Choi IH. The effects of sub-lethal concentration of silver nanoparticles on inflammatory and stress genes in human macrophages using cDNA microarray analysis. *Biomaterials* 2012, 33:4690–4699.
21. Eustaquio T, Leary JF. Nanobarcoding: detecting nanoparticles in biological samples using *in situ* polymerase chain reaction. *Int J Nanomed* 2012, 7:5625–5639.
22. Schwab F, Bucheli TD, Camenzuli L, Magrez A, Knauer K, Sigg L, Nowack B. Diuron sorbed to carbon nanotubes exhibits enhanced toxicity to *Chlorella vulgaris*. *Environ Sci Technol* 2013, 47:7012.
23. Murdock RC, Hussain SM. Radio frequency controlled stimulation of intracellular gold or silver nanoparticle conjugates for use as potential sensors or modulators of biological function. AFRL-RH-WP-TR-2010-0141, Air Force Research Laboratory, Biosciences and Protection Division, Applied Biotechnology Branch, 2010.
24. Carlson C, Hussain SM, Schrand AM, Braydich-Stolle LK, Hess KL, Jones RL, Schlager JJ. Unique cellular interaction of silver nanoparticles: size-dependent generation of reactive oxygen species. *J Phys Chem B* 2008, 112:13608–13619.
25. Park J, Park JH, Ock KS, Ganbold EO, Song NW, Cho K, Lee SY, Joo SW. Preferential adsorption of fetal bovine serum on bare and aromatic thiol-functionalized gold surfaces in cell culture media. *J Colloid Interface Sci* 2011, 363:105–113.
26. Santos T, Ferreira R, Maia J, Agasse F, Xapelli S, Cortes L, Bragança J, Malva JO, Ferreira L, Bernardino L. Polymeric nanoparticles to control the differentiation of neural stem cells in the subventricular zone of the brain. *ACS Nano* 2012, 6:10463–10474.
27. Chumakova OV, Liopo AV, Andreev VG, Cicenaite I, Evers BM, Chakrabarty S, Pappas TC, Esenaliev RO. Composition of PLGA and PEI/DNA nanoparticles improves ultrasound-mediated gene delivery in solid tumors *in vivo*. *Cancer Lett* 2008, 261:215–225.
28. Lee WM, Kwak JI, An YJ. Effect of silver nanoparticles in crop plants *Phaseolus radiatus* and *Sorghum bicolor*: media effect on phytotoxicity. *Chemosphere* 2012, 86:491–499.
29. Kwok KWH, Auffan M, Badireddy AR, Nelson CM, Wiesner MR, Chilkoti A, Liu J, Marinakos SM, Hinton DE. Uptake of silver nanoparticles and toxicity to early life stages of Japanese medaka (*Oryzias latipes*): effect of coating materials. *Aquat Toxicol* 2012, 120–121:59–66.
30. Kim SW, Nam SH, An YJ. Interaction of silver nanoparticles with biological surfaces of *Caenorhabditis elegans*. *Ecotoxicol Environ Saf* 2012, 77:64–70.
31. Rocha A, Zhou Y, Kundu S, González JM, BradleighVinson S, Liang H. *In vivo* observation of gold nanoparticles in the central nervous system of *Blaberus discoidalis*. *J Nanobiotechnol* 2011.
32. Husain M, Saber AT, Guo C, Jacobsen NR, Jensen KA, Yauk CL, Williams A, Vogel U, Wallin H, Halappanavar S. Pulmonary instillation of low doses of titanium dioxide nanoparticles in mice leads to particle retention and gene expression changes in the absence of inflammation. *Toxicol Appl Pharmacol* 2013, 269:250–262.
33. Ma JY, Mercer RR, Barger M, Schwegler-Berry D, Scabilloni J, Ma JK, Castranova V. Induction of pulmonary fibrosis by cerium oxide nanoparticles. *Toxicol Appl Pharmacol* 2012, 262:255–264.
34. Kotchey GP, Hasan SA, Kapralov AA, Ha SH, Kim K, Shvedova AA, Kagan VE, Star A. A natural vanishing act: the enzyme-catalyzed degradation of carbon nanomaterials. *Accounts Chem Res* 2012, 45:1770–1781.
35. Mercer RR, Hubbs AF, Scabilloni JF, Wang L, Battelli LA, Friend S, Castranova V, Porter DW. Pulmonary fibrotic response to aspiration of multi-walled carbon nanotubes. *Part Fibre Toxicol* 2011.
36. Sager TM, Wolfarth MW, Andrew M, Hubbs A, Friend S, Chen T, Porter DW, Wu N, Yang F, Hamilton RF, et al. Effect of multi-walled carbon nanotube surface modification on bioactivity in the C57BL/6 mouse model. *Nanotoxicology* 2014, 8:317–327.
37. Stapleton PA, Minarchick VC, Cumpston AM, McKinney W, Chen BT, Sager TM, Frazer DG, Mercer RR, Scabilloni J, Andrew ME, *et al.* Impairment of coronary arteriolar endothelium-dependent dilation after multi-walled carbon nanotube inhalation: a time-course study. *Int J Mol Sci* 2012, 13:13781–13803.
38. Badireddy AR, Budarz JF, Chellam S, Wiesner MR. Bacteriophage inactivation by UV-A illuminated fullerenes: role of nanoparticle-virus association and biological targets. *Environ Sci Technol* 2012, 46:5963–5970.
39. Zhang Q, Hitchins VM, Schrand AM, Hussain SM, Goering PL. Uptake of gold nanoparticles in murine macrophage cells without cytotoxicity or production of pro-inflammatory mediators. *Nanotoxicology* 2011, 5:284–295.
40. Grabinski C, Schaeublin N, Wijaya A, D'Couto H, Baxamusa SH, Hamad-Schifferli K, Hussain SM. Effect

of gold nanorod surface chemistry on cellular response. *ACS Nano* 2011, 5:2870–2879.

41. DeBrosse MC, Comfort KK, Untener EA, Comfort DA, Hussain SM. High aspect ratio gold nanorods displayed augmented cellular internalization and surface chemistry mediated cytotoxicity. *Mater Sci Eng C Mater Biol Appl* 2013, 33:4094.
42. Hutter E, Boridy S, Labrecque S, Lalancette-Hébert M, Kriz J, Winnik FM, Maysinger D. Microglial response to gold nanoparticles. *ACS Nano* 2010, 4: 2595–2606.
43. Sarlo K, Blackburn KL, Clark ED, Grothaus J, Chaney J, Neu S, Flood J, Abbott D, Bohne C, Casey K, et al. Tissue distribution of 20 nm, 100 nm and 1000 nm fluorescent polystyrene latex nanospheres following acute systemic or acute and repeat airway exposure in the rat. *Toxicology* 2009, 263:117–126.
44. Henry TB, Menn FM, Fleming JT, Wilgus J, Compton RN, Sayler GS. Attributing effects of aqueous C_{60} nano-aggregates to tetrahydrofuran decomposition products in larval zebrafish by assessment of gene expression. *Environ Health Perspect* 2007, 115:1059–1065.
45. Blanco E, Sangai T, Hsiao A, Ferrati S, Bai L, Liu X, Meric-Bernstam F, Ferrari M. Multistage delivery of chemotherapeutic nanoparticles for breast cancer treatment. *Cancer Lett* 2013, 334:245–252.
46. Bickford LR, Langsner RJ, Chang J, Kennedy LC, Agollah GD, Drezek R. Rapid stereomicroscopic imaging of HER2 overexpression in *ex vivo* breast tissue using topically applied silica-based gold nanoshells. *J Oncol* 2012.
47. Chaudhari K, Pradeep T. Spatiotemporal mapping of three dimensional rotational dynamics of single ultrasmall gold nanorods. *Sci Rep* 2014, 4: 5948–5964.
48. Jayachandran M, Litwiller RD, Owen WG, Heit JA, Behrenbeck T, Mulvagh SL, Araoz PA, Budoff MJ, Harman SM, Miller VM. Characterization of blood borne microparticles as markers of premature coronary calcification in newly menopausal women. *Am J Physiol Heart Circ Physiol* 2008, 295:H931–H938.
49. Jun Y-W, Sheikholeslami S, Hostetter DR, Tajon C, Craik CS, Alivisatos AP. Continuous imaging of plasmon rulers in live cells reveals early-stage caspase-3 activation at the single-molecule level. *Proc Natl Acad Sci USA* 2009, 106:17735–17740.
50. Vishnupriya S, Chaudhari K, Jagannathan R, Pradeep T. Single-cell investigations of silver nanoparticle-bacteria interactions. *Part Part Syst Charact* 2013, 30:1056–1062.
51. Weinkauf H, Brehm-Stecher BF. Enhanced dark field microscopy for rapid artifact-free detection of nanoparticle binding to *Candida albicans* cells and hyphae. *Biotechnol J* 2009, 4:871–879.
52. Lee ES, Oh YT, Youn YS, Nam M, Park B, Yun J, Kim JH, Song HT, Oh KT. Binary mixing of micelles using pluronics for a nano-sized drug delivery system. *Colloids Surf B Biointerfaces* 2011, 82:190–195.
53. Jayanna PK, Bedi D, Gillespie JW, DeInnocentes P, Wang T, Torchilin VP, Bird RC, Petrenko VA. Landscape phage fusion protein-mediated targeting of nanomedicines enhances their prostate tumor cell association and cytotoxic efficiency. *Nanomed Nanotechnol Biol Med* 2010, 6:538–546.
54. Yang X, Jiang C, Hsu-Kim H, Badireddy AR, Dykstra M, Wiesner M, Hinton DE, Meyer JN. Silver nanoparticle behavior, uptake, and toxicity in *Caenorhabditis elegans*: effects of natural organic matter. *Environ Sci Technol* 2014, 48:3486–3495.
55. Arnold MC, Badireddy AR, Wiesner MR, Di Giulio RT, Meyer JN. Cerium oxide nanoparticles are more toxic than equimolar bulk cerium oxide in *Caenorhabditis elegans*. *Arch Environ Contam Toxicol* 2013, 65:224–233.
56. Wang L, Castranova V, Mishra A, Chen B, Mercer RR, Schwegler-Berry D, Rojanasakul Y. Dispersion of single-walled carbon nanotubes by a natural lung surfactant for pulmonary *in vitro* and *in vivo* toxicity studies. *Part Fibre Toxicol* 2010, 7.
57. von der Kammer F, Ferguson PL, Holden PA, Masion A, Rogers KR, Klaine SJ, Koelmans AA, Horne N, Unrine JM. Analysis of engineered nanomaterials in complex matrices (environment and biota): general considerations and conceptual case studies. *Environ Toxicol Chem* 2012, 31:32–49.
58. Badireddy AR, Wiesner MR, Liu J. Detection, characterization, and abundance of engineered nanoparticles in complex waters by hyperspectral imagery with enhanced darkfield microscopy. *Environ Sci Technol* 2012, 46:10081–10088.
59. Sankar MU, Aigal S, Maliyekkal SM, Chaudhary A, Kumar AAA, Chaudhari K, Pradeep T. Biopolymer-reinforced synthetic granular nanocomposites for affordable point-of-use water purification. *Proc Natl Acad Sci USA* 2013, 110:8459–8464.
60. Badireddy AR, Budarz JF, Marinakos SM, Chellam S, Wiesner MR. Formation of silver nanoparticles in visible light-illuminated waters: mechanism and possible impacts on the persistence of AgNPs and bacterial lysis. *Environ Eng Sci* 2014, 31:338–349.

